

PACS numbers: 42.65.Ky; 79.20.Ds; 81.16.Rf
DOI: 10.1070/QE2009v039n07ABEH014118

Three-wave interactions of surface defect-deformation waves and their manifestations in the self-organisation of nano- and microstructures in solids exposed to laser radiation

V.I. Emel'yanov, D.M. Seval'nev

Abstract. **The self-organisation of the surface-relief nanostructures in solids under the action of energy and particle fluxes is interpreted as the instability of defect-deformation (DD) gratings produced by quasi-static Lamb and Rayleigh waves and defect-concentration waves. The allowance for the nonlocality in the defects – lattice atom interaction with a simultaneous account for both (normal and longitudinal) defect-induced forces bending the surface layer leads to the appearance of two maxima in the dependence of the instability growth rate of DD waves on the wave number. Three-wave interactions of quasi-static coupled DD waves (second harmonic generation and wave vector mixing) are considered for the first time, which are similar to three-wave interactions in nonlinear optics and acoustics and lead to the enrichment of the spectrum of surface-relief harmonics. Computer processing of experimental data on laser-induced generation of micro- and nanostructures of the surface relief reveals the presence of effects responsible for the second harmonic generation and wave vector mixing.**

Keywords: *surface defect-deformation waves, generation of harmonics, wave vector mixing, laser-induced nano- and microstructures.*

1. Introduction

Nonlinear interactions of three waves with frequencies ω_1, ω_2, ω_3 [second harmonic generation (SHG): $\omega_3 = \omega_1 + \omega_2$ ($\omega_1 = \omega_2$) and frequency mixing: $\omega_3 = \omega_1 \pm \omega_2$] are classical phenomena in nonlinear optics [1] and nonlinear acoustics [2]. In this paper, we show for the first time that there exist analogues of these nonlinear wave effects involving waves of a new type: surface quasi-static (with the zero frequency) defect-deformation (DD) waves excited during the interaction of laser radiation with solids. These effects include SHG of a surface relief: $q_3 = q_1 + q_2$ ($q_1 = q_2$) and wave vector mixing of DD gratings ($\boldsymbol{q}_3 = \boldsymbol{q}_1 \pm \boldsymbol{q}_2$). If the electronic anharmonicity is responsible for nonlinear-optical effects [1] and deformation anharmonicity is responsible for nonlinear-acoustic effects [2], the nonlinear interaction of DD waves considered in this paper can be explained by the DD anharmonicity caused by the interaction of defects with the self-consistent deformation field.

These new nonlinear laser-induced effects have not been studied experimentally so far; however computer processing of experimental data on laser-induced generation of micro- and nanostructures of the surface relief performed in this paper reveals the presence of effects, which can be interpreted as a SHG and wave vector mixing of DD waves.

A number of self-organisation processes of nano- and microstructures on the surfaces of solids are accompanied by the formation of a nanometre- or micrometre-thick layer saturated with mobile point defects: interstices, vacancies, electron – hole pairs and doping atoms. This situation appears, for example, when an ensemble of nanodots is produced due to the exposure of semiconductors and metals to laser and ion beams (see review [3]). The defect-saturated surface layer appearing due to irradiation has a grating constant, which differs from the grating constant of the low-lying crystal layer ('the substrate'). This leads to the appearance of mechanic stresses in the surface layer.

It is known that if the plane stressed (stretched) surface layer of thickness h is saturated with mobile point defects, then, when the critical concentration of defects is exceeded, the plane state becomes unstable and the layer undergoes a transition to the periodically bending state with a simultaneous accumulation of defects in the relief extrema [4 – 6]. In this case, the displacements of the medium inside the layer are given as in the case of the bending Lamb wave, while the displacements in the substrate are given as in the case of the Rayleigh wave [6, 7]. Coupled static Lamb – Rayleigh deformations in the layer and substrate produced due to the development of this DD instability, are maintained by the self-consistent distribution of point defects deforming the elastic continuum. This deformed state of the layer and substrate represents a static analogue of a dynamic Lamb – Rayleigh wave propagating in a thin surface layer with the density exceeding the substrate density [8].

The appearance of the periodic surface relief is accompanied by the accumulation of defects in its extrema. In this case, interstices are accumulated in the relief projections, while vacancies – in its hollows. This periodic modulation of the surface relief and the coupled grating of defect clusters compose a surface DD wave (grating), which is characterised by the wave vector $\boldsymbol{q}$ [6]. During the development of the DD instability the amplitudes of DD gratings increase in time as $\exp(\lambda_{\boldsymbol{q}} t)$, where $\lambda_{\boldsymbol{q}}$ is the growth rate. The value of $q = q_{\rm m}$, at which the growth rate maximum is achieved, determines the period of dominating gratings $\Lambda_{\rm m} = 2\pi/q_{\rm m}$ found in the Fourier spectrum of the surface relief. The

V.I. Emel'yanov, D.M. Seval'nev Department of Physics, M.V. Lomonosov Moscow State University, Vorob'evy gory, 119991 Moscow, Russia; e-mail: emelyanov.vladimir@gmail.com

Received 20 March 2009
Kvantovaya Elektronika **39** (7) 678 – 684 (2009)
Translated by I.A. Ulitkin

allowance for the nonlocality in the interaction of defects with lattice atoms in the expansion of the core of interaction operators to the terms of the fourth order inclusively with a simultaneous account for both (normal and longitudinal) defect-induced forces bending the layer leads, at a rather large excess over the instability threshold (at large enough excess of the critical concentration of defects), to the appearance of the second growth rate maximum $\lambda_{\boldsymbol{q}}$ for $q = q_{\rm c} = \pi/h$ [7] to which dominating gratings with the period $\Lambda_{\rm c} = 2\pi/q_{\rm c} = 2h$ correspond.

Superposition of dominating surface DD gratings with the vectors $\boldsymbol{q}$ different in value and direction produces a cellular seed DD structure on the isotropic surface [3]. The characteristic scale of inhomogeneities in it is determined by the period $\Lambda_{\rm m}$ (or $\Lambda_{\rm c}$). In the case of autoselection of directions of wave vectors $\boldsymbol{q}$ (due to the crystal or induced anisotropy of elastic moduli and diffusion coefficients or due to the processes of angular self-organisation on the isotropic surface [9]) on the surface, we deal either with two mutually perpendicular directions of vectors $\boldsymbol{q}$ (a rectangular grating [5]) or three directions oriented at angles 60° to each other (a hexagonal grating [9]). Therefore, depending on the threshold excess, either one DD wave with the wave vector $\boldsymbol{q}_{\rm m}$ or two waves with the wave vectors $\boldsymbol{q}_{\rm m}$ and $\boldsymbol{q}_{\rm c}$ are excited along the selected directions. Due to the nonlinear three-wave interaction between them, the SHG effects of the surface relief and wave vector mixing are possible during the development of the DD instability. Thus, this paper is devoted to the description of these effects and their observation in experimental data.

In the case of a rather intense laser or ion action, the seed DD structure (cellular, rectangular or hexagonal) is subjected to 'etching', the regions of defect clusters being etched with the velocity differing from the etching velocity of other regions. Etching 'visualises' the seed latent DD structure, which, in this manner, 'imposes' its periodicity and symmetry on the resultant permanent surface relief [3]. Due to this, it becomes possible, by using the Fourier transform of optical or AFM photographs of the surface with the reliefs produced upon irradiation, to reveal the effects of SHG and wave vector mixing of DD gratings, which was done for the first time in this paper.

2. Basic equations describing the DD instability of a stressed layer with mobile defects

Let the crystal surface layer of thickness h exposed to a laser or ion beam generate point defects with the concentration n_d ($d = {\rm v}$ for vacancies, $d = {\rm i}$ for interstices). The plane $z = 0$ coincides with the free surface of the sample and the z axis is directed from the surface inside the sample. We will write the defect concentration distribution in the layer in the form

$$n_d(x, y, z, t) = N_d(x, y, t) f(z), \tag{1}$$

where $N_d(x, y, t)$ is the concentration of defects on the surface $z = 0$; the function $f(z)$ specifying the defect distribution along the normal to the layer will be defined below [see expression (6)].

The equation for N_d has the form [7]

$$\frac{\partial N_d}{\partial t} = D_d \Delta N_d - \frac{D_d \theta_d}{k_{\rm B} T} \operatorname{div}[N_d \nabla(\xi + l_d^2 \Delta\xi + L_d^4 \Delta^2 \xi)]|_{z=0}, \tag{2}$$

where

$$\Delta = \frac{\partial^2}{\partial x^2} + \frac{\partial^2}{\partial y^2}; \quad \nabla = \hat{\boldsymbol{e}}_x \frac{\partial}{\partial x} + \hat{\boldsymbol{e}}_y \frac{\partial}{\partial y}; \quad \operatorname{div}\boldsymbol{A} = \frac{\partial A_x}{\partial x} + \frac{\partial A_y}{\partial y};$$

$\hat{\boldsymbol{e}}_x$ and $\hat{\boldsymbol{e}}_y$ are the unit vectors along the axes x and y, respectively; $\theta_d = \Omega_d K$ is the deformation potential of the defect; Ω_d is the change in the medium volume, when a defect is produced; K is the elasticity modulus; $\xi = \xi(x, y, z) = \operatorname{div}\boldsymbol{u}$ is the deformation in the layer; $\boldsymbol{u} = \boldsymbol{u}(x, y, z, t)$ is the vector of the medium displacement in the layer; D_d is the surface diffusion coefficient; T is the surface temperature. The parameters l_d^2 and L_d^4 describe the nonlocality of the defect–lattice atom interactions and are assumed specified parameters.

The film deformation ξ is described by the expression [10]

$$\xi(x, y, z, t) = -\nu\left(z - \frac{h}{2}\right)\Delta\zeta(x, y, t), \tag{3}$$

where $\nu = (1 - 2\sigma_{\rm P})/(1 - 2\sigma_{\rm P})$; $\sigma_{\rm P}$ is the Poisson coefficient of the film; ζ is the bending coordinate of the film (the displacement of points of the median plane along the z axis). The linear sign-alternating dependence of the deformation in the layer on the coordinate z (3) is a specific feature of the Lamb wave in the plates [8].

For the coordinate ζ, we will write the linear equation, which is obtained by generalising the ordinary equation of the free film bending from [10]:

$$\frac{\partial^2 \zeta}{\partial t^2} + l_0^2 c^2 \Delta^2 \zeta - \frac{\sigma_\parallel}{\rho_{\rm f}} \Delta\zeta$$

$$= -\sum_d \left[-\frac{\theta_d}{\rho_{\rm f} h} \int_0^h \frac{\partial n_d}{\partial z} {\rm d}z + \frac{\nu\theta_d}{\rho_{\rm f} h} \int_0^h \left(z - \frac{h}{2}\right) \Delta n_d \, {\rm d}z \right], \tag{4}$$

where $c^2 = E_{\rm f}/[\rho_{\rm f}(1 - \sigma_{\rm P}^2)]$ is the film rigidity coefficient; $E_{\rm f}$ is the Young coefficient; $l_0^2 = h^2/12$; $\sigma_\parallel$ and $\rho_{\rm f}$ is the longitudinal stress and film density. Note that the bending rigidity of the film (the coefficient in front of $\Delta^2\zeta$) depends on its thickness h, which plays the role of a scale parameter specific for the DD instability of the film.

In the left-hand side of (4) the term proportional to $\sigma_\parallel$ takes into account the effect of the isotropic longitudinal stress in the film appearing due to the mismatch of the grating parameters in the film and the substrate and (or) due to generation of defects in the surface layer. By assuming that $\sigma_\parallel > 0$, i.e. the film is experiencing the tensile stress, which is believed to be specified. The second term in the right-hand side of (4) takes into account the defect-induced bending force acting along the normal to the film surface and appearing due to the inhomogeneous distribution of defects along the z axis, and the third term in the right-hand side of (4) – the defect-induced bending longitudinal force appearing due to the inhomogeneous distribution of defects along the film. Note that in a more complete formulation of the problem it is necessary to take into account that the film bending results in the appearance of the displacement vector $\boldsymbol{u}$ in the substrate, which is given by the vector displacement components in the quasi-Rayleigh wave [7].

The allowance for the substrate reaction shows that this reaction can be neglected if the condition

$$\sigma_{\|} > \mu_{\mathrm{s}}\left(\Lambda_{\mathrm{m}}\,\frac{1-\beta_{\mathrm{s}}}{\pi h}\right) \tag{5}$$

is fulfilled, where $\beta_{\mathrm{s}} = c_{\mathrm{tr}}^2/c_{\mathrm{lt}}^2$; c_{lt} and c_{tr} are the longitudinal and transverse sound speed in the substrate; μ_{s} is the shear modulus in the substrate at the film–substrate interface. This condition can be fulfilled if the effective shear modulus at the interface is $\mu_{\mathrm{s}} \to 0$, for example, in the case of generation of misfit dislocations [11, 12] or due to the formation of vacancy clusters below the surface layer in the case of laser irradiation as a result of deformation-induced pumping of vacancies from the surface inside the medium [3]. Assuming this condition to be fulfilled, we will consider here the simplest model of a free film, i.e. the substrate reaction will be neglected.

In this case, the system of equations (2)–(4) and (1), if $f(z)$ is specified, is a closed system describing the DD instability of the stressed thin surface layer with mobile defects.

3. Equations for Fourier amplitudes; two maxima of the DD instability growth rate as functions of the wave number

It can be shown that because $h < \Lambda_{\mathrm{m}}$, n_d is rapidly adjusted to the distribution of the bending deformation with respect to z (3) and is an asymmetric (with respect to the point $z = h/2$) function of z:

$$n_d(x,y,z,t) = \frac{2}{h}\left(\frac{h}{2} - z\right)N_d(x,y,t). \tag{6}$$

It follows from (6) that

$$n_d(z=0) = -n_d(z=h) = N_d. \tag{7}$$

By substituting (6) into the right-hand side of (4) and calculating integrals taking (7) into account and by assuming that the deformation is adiabatically adjusted to the defect subsystem ($\partial^2\zeta/\partial t^2 = 0$), we obtain

$$\Delta^2\zeta - \frac{1}{l_{\|}^2}\,\Delta\zeta = -\sum_d\left(-A_d - \frac{2\nu\theta_d}{\rho_{\mathrm{f}}c^2h}\,\Delta\right)N_d, \tag{8}$$

where $A_d = 2\theta_d/(hl_0^2\rho_{\mathrm{f}}c^2)$ and the characteristic scale parameter is $l_{\|} = h[\rho_{\mathrm{f}}c^2/(12\sigma_{\|})]^{1/2}$.

By using the Fourier expansion, we obtain

$$\zeta(\boldsymbol{r},t) = \sum_{\boldsymbol{q}}\zeta_{\boldsymbol{q}}\exp(\mathrm{i}\boldsymbol{qr} + \lambda_{\boldsymbol{q}}t),$$
$$N_d(\boldsymbol{r},t) = \sum_{\boldsymbol{q}}N_d(\boldsymbol{q})\exp(\mathrm{i}\boldsymbol{qr} + \lambda_{\boldsymbol{q}}t). \tag{9}$$

Expressions (9) specify the superposition DD structure composed of coupled two-dimensional (cellular) DD gratings of the surface relief and defect concentration. In fact, each DD grating with the wave vector $\boldsymbol{q}$ is a bending static Lamb wave with the wavelength $\Lambda = 2\pi/q$ maintained by the self-consistent distribution of defects. It is possible to show that when the substrate reaction is taken into account, each quasi-static Lamb wave is related to the quasi-static Rayleigh wave in the substrate with the same wave vector $\boldsymbol{q}$ [6, 7]. The Fourier amplitudes of each DD grating with the wave vector $\boldsymbol{q}$ increase in time with the growth rate $\lambda_{\boldsymbol{q}}$. Summation in superpositions (9) is performed both over the directions and the modulus of vectors $\boldsymbol{q}$. In this case, summation over the modulus $|\boldsymbol{q}| = q$ is fulfilled within $q_1 \leqslant q \leqslant q_{\mathrm{c}}$, where $q_1 = \pi/L$ is the wave number of the first bending mode; L is the longitudinal surface dimension of the region with mobile defects; $q_{\mathrm{c}} = \pi/h$ is the wave number of the limiting bending mode [6].

By using (9), we obtain from expression (8) the linear coupling between $N_d(\boldsymbol{q})$ and $\zeta_{\boldsymbol{q}}$ in the DD grating with the wave vector q:

$$\zeta_{\boldsymbol{q}} = -\sum_d\frac{2\theta_d}{\rho_{\mathrm{f}}c^2hl_0^2}\left(1 + \nu l_0^2q^2\right)\left(q^4 + l_{\|}^{-2}q^2\right)^{-1}N_d(\boldsymbol{q}). \tag{10}$$

For simplicity, we retain in (10) the contribution of defects of only one type. By performing Fourier transform (2) and substituting (4), (10) into it, we obtain the equation for the Fourier amplitude:

$$\frac{\partial N_d(\boldsymbol{q})}{\partial t} = \lambda_{\boldsymbol{q}}N_d(\boldsymbol{q}) + D_d\,\frac{1}{N_{\mathrm{cr}}}\times\sum_{\boldsymbol{q}_1}\boldsymbol{qq}_1\,\frac{1 + \nu l_0^2q_1^2}{1 + l_{\|}^2q_1^2}\,N(\boldsymbol{q}_1)N(\boldsymbol{q} - \boldsymbol{q}_1), \tag{11}$$

where we set $l_d = 0$ and $L_d = 0$ in the linear term. The growth rate of the DD grating is

$$\lambda_{\boldsymbol{q}} = -D_dq^2 + D_dq^2\,\frac{N_{d0}}{N_{\mathrm{cr}}}\,\frac{\left(1 + \nu l_0^2q^2\right)\left(1 - l_d^2q^2 + L_d^4q^4\right)}{1 + l_{\|}^2q^2}, \tag{12}$$

where $N_{d0} = N_d(\boldsymbol{q} = 0)$ and the critical defect concentration $N_{\mathrm{cr}} = \sigma_{\|}k_{\mathrm{B}}T/(\nu\theta_d^2)$ is introduced.

To study dependence (12) numerically, it is convenient to pass to dimensionless variables $X = l_{\|}q$ and $\lambda_X = \lambda_{\boldsymbol{q}}l_{\|}^2/D_d$, parameters $a = l_0^2/l_{\|}^2$, $b = l_d^2/l_{\|}^2$, $g = L_d^4/l_{\|}^4$ and to introduce the governing parameter $\varepsilon = N_{d0}/N_{\mathrm{cr}}$. Using these notation, we have

$$\lambda_X = -X^2 + X^2\varepsilon\left(1 + a\nu X^2\right)\frac{1 - bX^2 + gX^4}{1 + X^2}. \tag{13}$$

The dependences of the growth rate λ_X on X for two governing parameters ($\varepsilon = 5$ and 10) are presented in Fig. 1. While plotting the dependences we used dimensionless

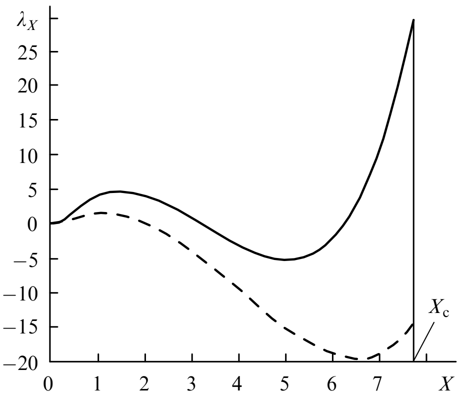

Figure 1. Dependences of the dimensionless growth rate λ_X' of the Fourier amplitude of the DD grating on the dimensionless wave number X for the control parameter $\varepsilon = 5$ (dashed curve) and 10 (solid curve); $X_{\mathrm{c}} = l_{\|}q_{\mathrm{c}}$ is the reduced wave number of the limiting bending mode.

parameters $a = 1.4 \times 10^{-2}$, $b = 1.5 \times 10^{-2}$ and $g = 1.8 \times 10^{-3}$, which can be obtained, for example, at the following physical parameters typical for the nanostructure formation: $h = 10^{-6}$ cm, $\rho_f c^2 = 7 \times 10^{11}$ erg cm^{-3}, $\sigma_\parallel = 10^{10}$ erg cm^{-3}, $l_d = 3 \times 10^{-7}$ cm and $L_d = 5 \times 10^{-7}$ cm.

One can see from Fig. 1 that at the defect concentration exceeding the threshold value, the growth rate first has one positive maximum at $q = q_m$ (the period of the DD grating corresponding to it is $\Lambda = \Lambda_m = 2\pi/q_m$) and in the case of larger concentrations, apart from the maximum at $\Lambda = \Lambda_m$, there appears an additional positive maximum in the short-wavelength region at

$$|\boldsymbol{q}_c| = \pi/h \quad (\Lambda = \Lambda_c = 2h). \tag{14}$$

Thus, two DD gratings with the wave vectors $\boldsymbol{q} = \boldsymbol{q}_m$ and $\boldsymbol{q} = \boldsymbol{q}_c$ have the maximum growth rate.

The long-wavelength maximum of the growth rate at $\Lambda = \Lambda_m$ (for $q = q_m$) can be described analytically if we neglect the nonlocality of the DD interaction in (12) by setting $l_d = L_d = 0$ and, in addition, neglect the longitudinal bending force ($\nu l_0^2 q^2 < 1$). Then, we obtain from (12)

$$\lambda_{\boldsymbol{q}} = -D_d q^2 + D_d q^2 \frac{N_{d0}}{N_{cr}} \frac{1}{1 + l_\parallel^2 q^2}. \tag{15}$$

The growth rate $\lambda_{\boldsymbol{q}}$ achieves the maximum value λ_m at $q = q_m$. In this case,

$$q_m = \frac{1}{l_\parallel} \left[\left(\frac{N_{d0}}{N_{cr}} \right)^{1/2} - 1 \right]^{1/2}, \tag{16}$$

$$\begin{aligned} \lambda_m &= D_d q_m^2 \left[\left(\frac{N_{d0}}{N_{cr}} \right)^{1/2} - 1 \right] \\ &= \frac{D_d}{l_\parallel^2} \left[\left(\frac{N_{d0}}{N_{cr}} \right)^{1/2} - 1 \right]^2 \operatorname{sign} \left[\left(\frac{N_{d0}}{N_{cr}} \right)^{1/2} - 1 \right]. \end{aligned} \tag{17}$$

One can see from (16), (17) that when the critical concentration of defects ($N_{d0}/N_{cr} > 1$) is exceeded, the value of q_m becomes real and simultaneously the growth rate λ_m becomes positive. At $T = 300$ K, $\sigma_\parallel = 10^{10}$ erg cm^{-3}, $\theta_d = 10^2$ eV, $\nu = 0.5$, we obtain from (12) the estimate of the critical concentration: $N_{cr} = 2 \times 10^{16}$ cm^{-3}.

4. Thee-wave interactions of DD gratings

4.1 Equations of three-wave DD interactions

Consider now the nonlinear regime. We will restrict ourselves to the interaction of three DD gratings with the collinear wave vectors $\boldsymbol{q}_1 = \boldsymbol{q}_c$, $\boldsymbol{q}_2 = \boldsymbol{q}_m$ and $\boldsymbol{q}_3 = -(\boldsymbol{q}_c + \boldsymbol{q}_m)$. In particular, as wave vectors $\boldsymbol{q}_c$ and $\boldsymbol{q}_m$, we can use wave vectors given by expressions (14) and (16) for which the growth rate maximum $\lambda_{\boldsymbol{q}}$ is achieved.

Expressions for the Fourier amplitudes of interacting gratings follow from (11) and assume the form

$$\begin{aligned} \frac{\partial N(\boldsymbol{q}_m)}{\partial t} &= \lambda_{\boldsymbol{q}_m} N(\boldsymbol{q}_m) + D_d \frac{A_m}{N_{cr}} N(\boldsymbol{q}_c + \boldsymbol{q}_m) N(-\boldsymbol{q}_c), \\ \frac{\partial N(\boldsymbol{q}_c)}{\partial t} &= \lambda_{\boldsymbol{q}_c} N(\boldsymbol{q}_c) + D_d \frac{A_c}{N_{cr}} N(\boldsymbol{q}_c + \boldsymbol{q}_m) N(-\boldsymbol{q}_m), \\ \frac{\partial N(\boldsymbol{q}_c + \boldsymbol{q}_m)}{\partial t} &= \lambda_{\boldsymbol{q}_c + \boldsymbol{q}_m} N(\boldsymbol{q}_c + \boldsymbol{q}_m) \\ &\quad + D_d \frac{A_{cm}}{N_{cr}} N(\boldsymbol{q}_c) N(\boldsymbol{q}_m), \end{aligned} \tag{18}$$

where the coefficients of the three-wave DD interaction are

$$\begin{aligned} A_m &= -\boldsymbol{q}_c \boldsymbol{q}_m \frac{1 + \nu l_0^2 q_c^2}{1 + l_\parallel^2 q_c^2} + (\boldsymbol{q}_c + \boldsymbol{q}_m) \boldsymbol{q}_m \frac{1 + \nu l_0^2 (\boldsymbol{q}_c + \boldsymbol{q}_m)^2}{1 + l_\parallel^2 (\boldsymbol{q}_c + \boldsymbol{q}_m)^2}, \\ A_c &= -\boldsymbol{q}_m \boldsymbol{q}_c \frac{1 + \nu l_0^2 q_m^2}{1 + l_\parallel^2 q_m^2} + (\boldsymbol{q}_c + \boldsymbol{q}_m) \boldsymbol{q}_c \frac{1 + \nu l_0^2 (\boldsymbol{q}_c + \boldsymbol{q}_m)^2}{1 + l_\parallel^2 (\boldsymbol{q}_c + \boldsymbol{q}_m)^2}, \\ A_{cm} &= \boldsymbol{q}_m (\boldsymbol{q}_c + \boldsymbol{q}_m) \frac{1 + \nu l_0^2 q_m^2}{1 + l_\parallel^2 q_m^2} \\ &\quad + \boldsymbol{q}_c (\boldsymbol{q}_c + \boldsymbol{q}_m) \frac{1 + \nu l_0^2 \boldsymbol{q}_c^2}{1 + l_\parallel^2 \boldsymbol{q}_c^2}. \end{aligned} \tag{18$'$}$$

By passing in (18) to real variables $N_j = n_j \exp(i\varphi_j)$, we have a system of three equations for the real amplitudes n_j ($j =$ c, m, cm) and the equation for the phase difference $\Phi = \varphi_c + \varphi_m - \varphi_{cm}$:

$$\begin{aligned} \frac{\partial n_m}{\partial t} &= \lambda_m n_m + D_d A_m \frac{n_c n_{cm}}{N_{cr}} \cos \Phi, \\ \frac{\partial n_c}{\partial t} &= \lambda_c n_c + D_d A_c \frac{n_m n_{cm}}{N_{cr}} \cos \Phi, \\ \frac{\partial n_{cm}}{\partial t} &= \lambda_{cm} n_{cm} + D_d A_{mc} \frac{n_m n_c}{N_{cr}} \cos \Phi, \end{aligned} \tag{19}$$

$$\frac{\partial \Phi}{\partial t} = -\frac{D_d}{N_{cr}} \left(A_m \frac{n_c n_{cm}}{n_m} + A_c \frac{n_m n_{cm}}{n_c} + A_{mc} \frac{n_m n_c}{n_{cm}} \right) \sin \Phi. \tag{20}$$

Expression (20) describes the phase relaxation: $\Phi \to 0$. One can see from the comparison of expressions (20) and (19) that the ratio of the characteristic relaxation time of phases to the characteristic time of the defect transfer from one DD grating to others is $\tau_{ph}/\tau_0 \sim n_j/N_{cr} \sim n_j/N_{d0} \ll 1$. Therefore, in considering nonlinear transformation of DD gratings in (19), we can set $\Phi = 0$.

4.2 Second harmonic generation of the surface relief

Consider one of the DD gratings. When the DD instability threshold is slightly exceeded and the growth rate of DD gratings has only one maximum, this will be the DD grating with the wave vector q_m (16). We will show that due to three-wave interactions, summation of two identical wave numbers is possible: $q_{mm} = -q_m - q_m$. As a result, one more DD grating with the wave number $2q_m$ is generated on the surface of the initial grating with q_m. This case corresponds to the optical SHG process in a nonlinear crystal, if the exact phase-matching conditions are fulfilled. Expressions for coupling coefficients (18$'$) in this case have the form:

$$A_m = q_m^2 \frac{1 - 2 l_\parallel^2 q_m^2}{(1 + l_\parallel^2 q_m^2)(1 + 4 l_\parallel^2 q_m^2)}, \quad A_{mm} = \frac{4 q_m^2}{1 + l_\parallel^2 q_m^2}.$$

To solve system (19) numerically, we will pass to dimensionless time $t' = \lambda_{\rm m} t$, amplitudes $n'_j = n_j/N_{\rm cr}$ and parameters $A'_j = A_j l_\parallel^2$ and $\lambda'_{\boldsymbol q} = \lambda_{\boldsymbol q} l_\parallel^2 / D_d$ as well as set $\Phi = 0$. Then, for the SHG under study, the system of equations (19) takes the form

$$\frac{\partial n'_{\rm m}}{\partial t'} = n'_{\rm m} + \frac{A'_{\rm m}}{\lambda'_{\rm m}} n'_{\rm m} n'_{\rm mm},$$
$$\frac{\partial n'_{\rm mm}}{\partial t'} = \frac{\lambda'_{\rm mm}}{\lambda'_{\rm m}} n'_{\rm mm} + \frac{A'_{\rm mm}}{\lambda'_{\rm m}} n'_{\rm m} n'_{\rm m}. \tag{21}$$

The results of the numerical solution of this system for the initial conditions $n'_{\rm m}(t=0) = 0.5$, $n'_{\rm mm}(t=0) = 10^{-5}$ are presented in Fig. 2a. The values of growth rates $\lambda'_{\rm m}$ and $\lambda'_{\rm mm}$ are calculated by using expression (13) for $a = 1.4 \times 10^{-2}$, $b = 4 \times 10^{-5}$, $g = 10^{-8}$, $\varepsilon = 10$, and $v = 0.5$. The coupling coefficients $A'_{\rm m} = -0.22$, $A'_{\rm mm} = 2.8$ are calculated by using expression (18$'$). One can see that during the time exceeding the characteristic time of the linear amplitude growth of the first harmonic ($1/\lambda'_{\rm m}$), the amplitude of the second harmonic due to SHG starts exceeding the amplitude of the first harmonic (the linear amplitude growth of the second harmonic at this $\lambda'_{\rm mm}$ can be neglected because $\lambda'_{\rm m}/\lambda'_{\rm mm} = 11.5$ for the parameters used).

4.3 Wave vector mixing

Let us have initially two collinear DD gratings with the wave vectors $q_1 = q_{\rm m}$ and $q_2 \equiv q_{\rm c} = 2q_{\rm m}$. Consider the process of the wave vector mixing due to which there appears a grating with the wave number $q_3 \equiv q_{\rm cm} = -(q_1 + q_2) = -3q_{\rm m}$. In this case, in dimensionless variables and at $\Phi = 0$, system (19) assumes the form

$$\frac{\partial n'_{\rm m}}{\partial t'} = n'_{\rm m} + \frac{A'_{\rm m}}{\lambda'_{\rm m}} n'_{\rm c} n'_{\rm cm}, \quad \frac{\partial n'_{\rm c}}{\partial t'} = \frac{\lambda'_{\rm c}}{\lambda'_{\rm m}} n'_{\rm c} + \frac{A'_{\rm c}}{\lambda'_{\rm m}} n'_{\rm m} n'_{\rm cm},$$
$$\frac{\partial n'_{\rm cm}}{\partial t'} = \frac{\lambda'_{\rm cm}}{\lambda'_{\rm m}} n'_{\rm cm} + \frac{A'_{\rm cm}}{\lambda'_{\rm m}} n'_{\rm m} n'_{\rm c}. \tag{22}$$

The results of the numerical solution of the system of equations (22) at $\lambda'_{\rm cm}/\lambda'_{\rm m} = -2$, $\lambda'_{\rm m}/\lambda'_{\rm c} = 11.5$ are shown in Fig. 2b for initial conditions $n'_{\rm m}(t{=}0){=}0.25$, $n'_{\rm c}(t{=}0){=}1$, $n'_{\rm cm}(t{=}0) = 10^{-5}$. The growth rates are calculated by using (13) at $a = 1.4 \times 10^{-2}$, $b = 4 \times 10^{-5}$, $g = 10^{-8}$, $\varepsilon = 10$, and $v = 0.5$. The coupling coefficients $A'_{\rm m} = -0.12$, $A'_{\rm c} = -0.7$ and $A'_{\rm cm} = 3.5$ are calculated by using (18$'$). One can see that even in the case of the negative growth rate of the third harmonic, we observe a significant increase in its amplitude due to the nonlinear transformation.

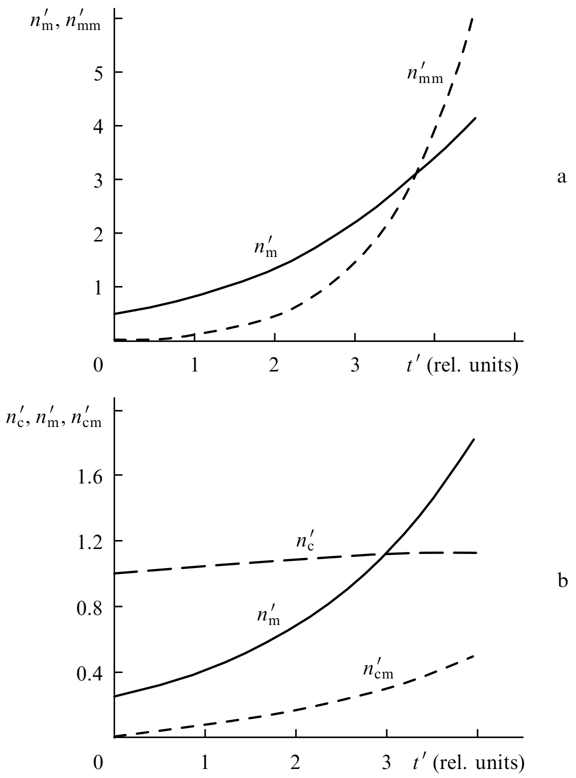

Figure 2. Amplitudes of the first ($n'_{\rm m}$) and second ($n'_{\rm mm}$) harmonics calculated by expressions (21) for the parameters specified in the text (a) and amplitudes of the first ($n'_{\rm m}$), second ($n'_{\rm c}$) and third ($n'_{\rm cm}$) harmonics of the surface relief calculated by expressions (22) for the parameters specified in the text (b) as functions of dimensionless time t'.

5. Comparison of the theory with experimental results

In paper [13] the surface of the (100) crystalline silicon was irradiated by linear polarised millisecond pulses from a neodymium laser with the energy density near the melting threshold. Irradiation in the case of the normal incidence of laser radiation on the sample resulted in the formation of a two-dimensional crystallographically oriented grating of the surface relief with a micrometre period, whose characteristics are described by the theory of the surface DD instability [5, 13]. At the angle of incidence 30°, the relief had a more complicated shape, which did not allow such an unambiguous interpretation (Fig. 3). Large-scale (~ 30 μm) crystallographically oriented blocks are interpreted in paper [14] as a result of the development of a thermal-deformation instability and, in this case, present no interest.

Of interest is a comparatively small-scale (micrometre) relief. The Fourier transform of this relief (Fig. 3) shows that this complex micrometre relief is produced by the superposition of three gratings. One grating with the wave vector parallel to the field strength vector $\boldsymbol{E}$ of the exciting radiation and with the period depending on the angle of incidence is produced due to the development of the interference instability [15]. Two other crystallographically oriented gratings with the period 3.5 μm and the wave vectors $\boldsymbol{q}_{\rm m}$ along the mutually perpendicular directions of type [100] are produced due to the development of the surface DD instability [5, 13]. The period of these DD gratings is independent of the angle of radiation incidence. In addition, intense crystallographically oriented maxima, corresponding to two mutually perpendicular relief gratings with the wave numbers $2|\boldsymbol{q}_{\rm m}|$, can be clearly seen, which indicates the SHG of the relief. A more detailed study of the photograph shows that the DD grating consists of two periodically repeated dark lines and a grey line between them. It is this pattern that is obtained in computer simulations of a two-dimensional image of the surface relief in the presence of the first and second harmonics (Figs 4b and d).

In paper [16], when Ge was irradiated by $\tau_{\rm p} \sim$ 1-μs, 0.53-μm laser pulses, the laser scanning regime was used inside

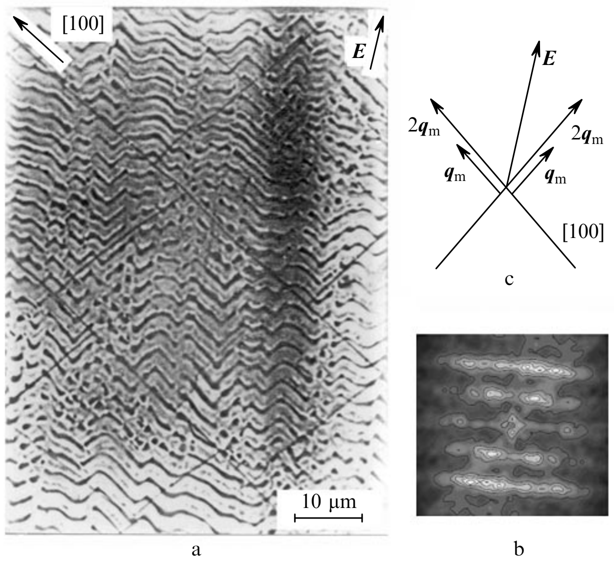

Figure 3. Photograph of the (100) Si surface irradiated by a millisecond pulse of linearly polarised radiation, which was obtained with an optical microscope [13] (a), the Fourier transform of the surface relief (each pair of the maxima lying on the diameter and equidistant from the centre corresponds to one relief grating) (b) and the directions of vectors $\boldsymbol{q}_{\mathrm{m}}$ and $2\boldsymbol{q}_{\mathrm{m}}$ of DD gratings and the electric field strength vector $\boldsymbol{E}$ of exciting radiation (c).

the rectangular regions of size 3×5 mm. Inside each scanning region the densities of the incident energy F were fixed at the constant number of radiation pulses falling on each point of the surface, $N = 10^3$ (i.e. the total irradiation time of each point was about a millisecond). On passing from one scanning region to another, only the energy density F in each pulse changed. These changes occurred near the threshold energy density of inelastic deformation $F_0 \sim 0.1$ J cm^{-2}, the characteristic irradiation intensities being $\sim 10^5 - 10^6$ W cm^{-2}. As the radiation dose was increased, the formation of a disordered ensemble of nanoclusters was first observed, then an ordered two-dimensional nanocluster grating was formed, which was oriented along the sides of the rectangular region being scanned (Fig. 4a), and then a one-dimensional nanograting appeared. The DD theory of this effect describing these transitions and nanostructure parameters was constructed in papers [17, 18].

The shape of the obviously nonmonochromatic periodic surface nanorelief recorded with the help of the profilometer (Fig. 4b) has remained unexplained till recently. The key to the explanation follows from the fact that in summing the first and second spatial harmonics, there appears a relief approximately corresponding to the experimental one. A better correspondence of the modelled relief to the experimental one is obtained by summing the first, second and third harmonics (cf. Figs 4d and b). The Fourier transform of the experimental relief presented in Fig. 4b shows that the first, second and third harmonics of the relief are really dominating in the spectrum (Fig. 4c).

6. Conclusions

Thus, the study performed in this paper (see also [7]) shows

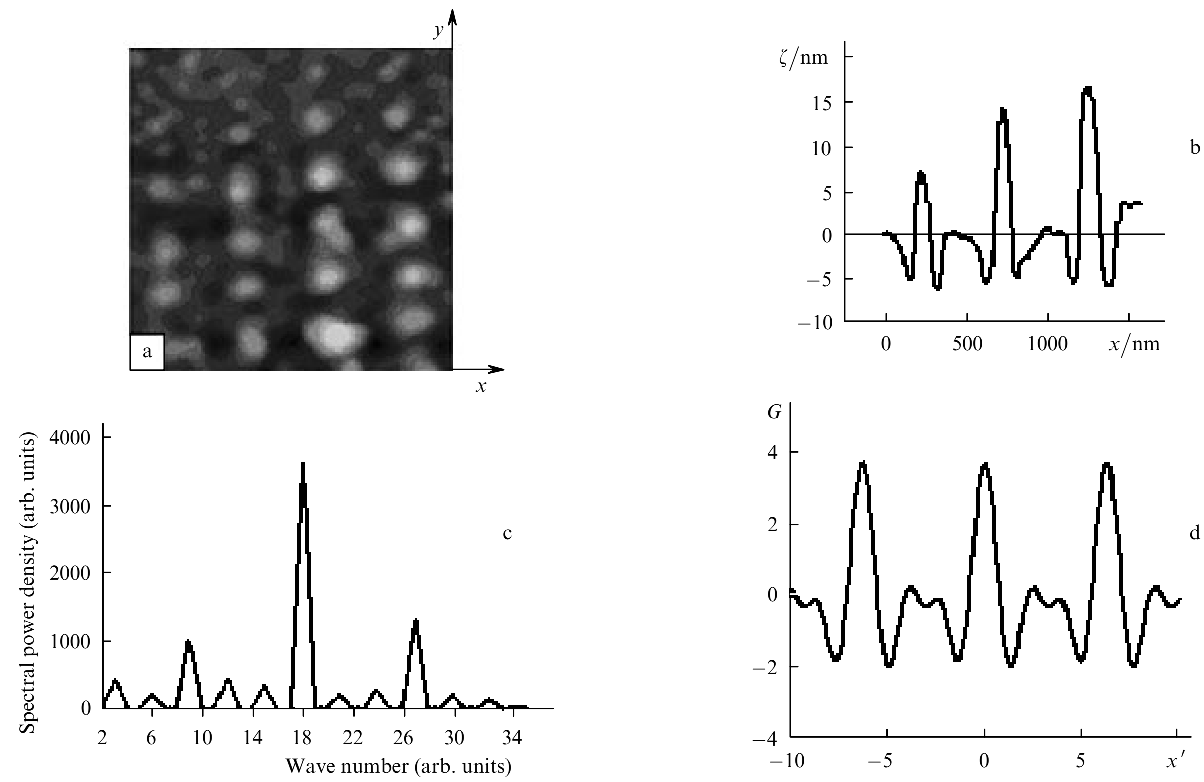

Figure 4. AFM photograph of the Ge surface after irradiation (a), the surface relief $\zeta(x)$ along the x axis recorded with a profilometer [16] (b), the spectral power density $|\zeta_q|^2$ of the surface relief shown in Fig. 4b (by neglecting the large-scale modulation) (c) and the function $G(x') = \cos x' + 1.7\cos(2x' + 0.1) + \cos 3x'$ reproducing the profilogram $\zeta(x)$ without taking into account the large-scale modulation (d). The amplitudes of the harmonics in the superposition $g(x')$ correspond to $|\zeta_q|^2$.

that the surface relief produced due to the development of the DD instability can contain in the linear regime, depending on the excess over the threshold, either one or two dominating harmonics with the wave vectors $\boldsymbol{q}_{\rm m}$ (16) and $\boldsymbol{q}_{\rm c}$ (14). In both cases, the modulation period of the relief is approximately equal to the thickness of the defect-enriched layer produced upon laser (in the general case – beam) irradiation, the thickness lying in the nanometre or micrometre range [3]. In the nonlinear regime, there can appear additional harmonics with the wave vectors $2\boldsymbol{q}_{\rm m}$, $3\boldsymbol{q}_{\rm m}$, $\boldsymbol{q}_{\rm c} - \boldsymbol{q}_{\rm m}$ considered in this paper as well as other harmonics generated by other three-wave interactions.

The physical mechanism of harmonic generation in the case of the DD instability consists in the spatial redistribution of defects under the action of self-consistent deformation grating on the initial defect grating. For example, during the SHG, the defect grating with the wave vector $\boldsymbol{q}_{\rm m}$ is affected by the grating of the deformation-induced forces with the same wave vector $\boldsymbol{q}_{\rm m}$ but phase shifted by $\pi/2$. This leads to the appearance of the grating of defect fluxes with the wave vector $2\boldsymbol{q}_{\rm m}$, which serves as a source in equation (2) for the defect concentration [or, in the Fourier transform, in expression (11)]. Therefore, the nonlinear (quadratic) defect flux in the case of the SHG of the surface relief is analogues to the quadratic polarisation of the medium (or current) in the case of generation of the second optical harmonic.

The presence of two maxima of the growth rate and the possibility of nonlinear generation of DD harmonics of the relief should be taken into account in the analysis of the experimental data on the generation of the surface relief appearing due to irradiation of solids. Thus, the appearance of two modulation scales of the relief is a typical feature of the generation processes of nano- and microstructures in laser and ion etching of semiconductor surfaces [3]. Three-wave interactions, as shown in this paper, lead to the SHG. It can be expected that at even larger excesses over the threshold, the consideration of higher-order nonlinear interactions will result in a further enrichment of the spectrum of surface-relief harmonics.

References

1. Akhmanov S.A., Khokhlov R.V. *Problems of Nonlinear Optics* (New York: Gordon and Breach, 1972; Moscow: Izd. VINITI, 1965).
2. Rudenko O.V., Soluyan S.I. *Theoretical Foundations of Nonlinear Acoustics* (New York: Plenum Press, 1977; Moscow: Nauka, 1975).
3. Emel'yanov V.I. *Laser Phys.*, **18**, 682 (2008).
4. Emel'yanov V.I., in *Nelineinye volny (lektsii na VII Vsesoyuznoi shkole po nelineinym volnam, Gor'kii, 1987)* [Nonlinear Waves (Lectures at the VII All-Union School on Nonlinear Waves, Gorky, 1987] (Moscow: Nauka, 1989) p. 198.
5. Emel'yanov V.I. *Laser Phys.*, **2**, 389 (1992).
6. Emel'yanov V.I. *Kvantovaya Elektron.*, **28**, 2 (1999) [*Quantum Electron.*, **29**, 561 (1999)].
7. Emel'yanov V.I. *Laser Phys.*, **18**, 1435 (2008).
8. Viktorov I.A. *Zvukovye poverkhnostnye volny v tverdykh telakh* (Surface Sound Waves in Solids) (Moscow: Nauka, 1981).
9. Emel'yanov V.I., Mikaberidze A.I. *Phys. Rev. B*, **72**, 235407 (2005).
10. Landau L.D., Lifshitz E.M. *Theory of Elasticity* (Oxford: Pergamon Press, 1979; Moscow: Nauka, 1987).
11. Bottani C.E., Yakona M. *J. Phys.: Condens. Matter*, **1**, 8337 (1989).
12. Dodson B.W., Tsao J.Y. *Appl. Phys. Lett.*, **51**, 1325 (1987).
13. Banishev A.F., Emel'yanov V.I., Novikov M.M. *Laser Phys.*, **2**, 178 (1992).
14. Emel'yanov V.I., Eremin K.I. *Kvantovaya Elektron.*, **31**, 154 (2001) [*Quantum Electron.*, **31**, 154 (2001)].
15. Akhmanov S.A., Emel'yanov V.I., Koroteev N.I., Seminogov V.N. *Usp. Fiz. Nauk*, **147**, 675 (1985).
16. Vintsents S.V., Zaitsev A.V., Plotnikov G.S. *Fiz. Tekh. Poluprovodn.*, **37**, 134 (2003).
17. Emel'yanov V.I., Vintsents S.V., Plotnikov G.S. *Poverkhnost*, (11), 55 (2007).
18. Emel'yanov V.I., Zaitsev A.V., Plotnikov G.S. *Poverkhnost*, (5), 1 (2008).